Some Methods of Signal Processing and Beamforming in Hydrographic Applications

T. Ruuben, J. Derkats

Department of Radio and Communication Engineering, Tallinn University of Technology,
Ehitajate str. 5, 19086 Tallinn, Estonia, phone: +3726202350; e-mail: truuben@lr.ttu.ee, juliad@lr.ttu.ee

Introduction

Without constant updating of hydrographical data it is not possible to provide safe navigation, especially in coastal and harbour areas. Thus, high quality maps and charts require that standard measurement methods be improved. Hydrographical data is based on a sonar measurement collection in a passive or active way. The bathymetry survey data always has uncertainty caused by survey vessel positioning, depth measurement precision (measurement accuracy, seafloor material parameters, etc), processing methods of collected data including the correction of the sound velocity and data post-processing and representation.

The fast signal processing development at the hardware level would affect not only data collecting and post-processing areas, but will also provide new opportunities for the measurement precision studies. For an active sonar system, the measurement accuracy could be increased by the use of the spread spectrum sounding signals and the appropriate beamforming and processing methods. Since processing depends on the practical measurement method, the equivalent distance sensor array model, as one of the possible sonar system solutions, is chosen to show the dynamics of the studied signals. Firstly, this paper reviews of the hydrographic standards and depth uncertainty values. Secondly, the examples of additional sounding signals and the optimum reception algorithms will be presented. Finally, advanced FFT beamforming modelling results will be compared with the block-phase beamforming method results.

Standards for hydrographic surveys

The standards for hydrographic surveys, issued by the International Hydrographic Organisation (IHO) [1], provide classifications of the different types of surveys, including the depth uncertainty specifications. Other standards have minor distribution, but nevertheless declare higher demands for the standard uncertainty level and must be taken into account as a goal for real measurement system implementation and modelling studies. Those standards are:

- The International Hydrographic Organisation S44 standard
- The Swedish Maritime Administration (SMA) Exclusive Order standard
- The US Army Corps of Engineers shallow water standards (USACE)
- The Land Information New Zealand Standards for deep water multibeam echosounder surveys (LINZ)
- International Marine Contractors Association standards (IMCA)

The IHO S44 4th Edition classifies four different types of survey data: Special Order, Order 1, 2 and 3.
According to the S-44 the error limits for depth accuracy could be calculated by the formula

$$\hat{d} = \sqrt{a^2 + (b \cdot d)^2} \quad \text{(m)},$$

where a – constant depth error, i.e. the sum of all constant errors; $b \cdot d$ – depth dependent error, i.e. the sum of all depth dependent errors; b – factor of a depth dependent error; d – depth.

The values of a and b listed in the S-44 correspond to the survey data orders. The following figure shows the summary of standards for hydrographic surveys and numerical values of the depth accuracy limits.

Obviously the S-44 Special Order (Fig. 1), is the most demanding order of IHO surveys covers the specific critical areas with minimum underkeel clearance and where bottom characteristics are potentially hazardous to vessels. Examples are harbours, berthing areas, and associated critical channels. Special Order requires the use of closely spaced lines in conjunction with a side scan sonar, multi-transducer arrays or high resolution multibeam echosounders to obtain 100% bottom search. It must be ensured that cubic features greater than 1m can be discerned by the sounding equipment.

According to the standard the horizontal accuracy (95% Confidence Level) must be up to 2 m, depth accuracy for reduced depths $a = 0.25$ (m). $b = 0.0075$, system detection capability cubic features > 1 m [3].
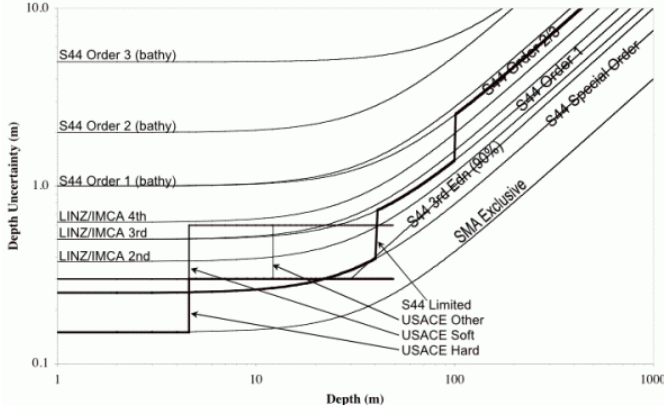
Fig. 1. Hydrographic standards and depth uncertainty [2]

With regard to the existing standard limits, in the development of new methods the most critical condition as the starting point, for example, the SMA Exclusive limit, that could lead to the future IHO standard improvements, must be taken into account.

This paper considers the sensor array as one of the possible modeling solutions to increase system resolution at a physical level and at the same time to use the sounding impulse power in a more effective way.

The phase coded sounding signals

Since the processing of a long coded pulse echo would give us a relatively narrow pulse and as a result not only more efficient use of the average power but also could improve resolution capability. The main compression selection parameters are the range coverage, the sidelobe levels at reception and signal to noise ratio. To study the possible real system improvements, the widely used binary phase-coded waveforms were used. The signal is subdivided into a number of subpulses of equal duration with the particular phase. The phase values could be obtained from the optimal binary sequences whose peak sidelobe values of the autocorrelation function are minimum possible for a given code length.[4] In practice, the widely used Barker code values or pseudorandom noise sequences, for example, the LFSR (linear-feedback shift-register) sequences, could be the reasonable choice, as the reception is implemented by the matched filtering or the correlation processing. Concerning the limited number and the length of Barker codes, the nested Barker codes [5] allow us to increase the system resolution at the same power level. Moreover, properties of those codes would lead us to the narrow peak at zero-doppler response and provide the resolution increase at the optimal filter output.[6] In this case the resolution is determined by the signal chip length, and could be improved k times, where k is the number of signal chips (elements). Here, the resolution in a simple pulse waveform case is determined by the whole signal length.[5]

For example, we use the 5-element (chip) nested Barker code. To obtain a desirable sounding signal, we fix amplitude value on the τ_e interval and phase values will be

$\Delta\phi \in \{0°, 180°\}$. So as a result we have a physical binary phase manipulated signal, where phase changes are made according to the values of the 5-element Barker code. The number of signal chips will be 25. Figure 2 shows the ideal optimal filter output for the nested 5-element Barker code.
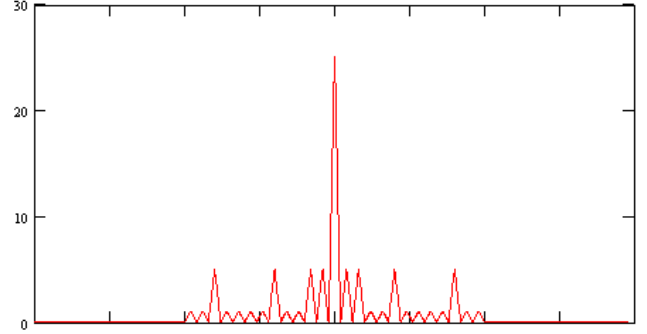

Fig. 2. Vertical cut $\Psi(\tau,0)$ (zero-doppler) of the ambiguity function $\Psi(\tau,F)$ [7] of the nested 5-element Barker code

The reception model of the array system includes the beamforming algorithms and the optimal reception. So, the dynamics of the sample signals in equivalent distance sensor array must be studied. The use of the Barker codes with the phase compensation in an original way has some strong limitation when the received signals are at the directions deflected from the normal.[8] Some additional beamforming methods should be used for the signals, formed with the optimal binary sequences.

The dynamics of scanning signals in equivalent distance sensor array

In general, we are interested only in independent partial directions [9], i.e. $\beta = \beta_\gamma$ and array output signal is expressed by

$$\overset{o}{y}(\beta_\gamma,l) = \sum_{n=0}^{N-1}\sum_{k=0}^{KT-1} a(l - k\tau_e - nd \cdot \sin\beta_\gamma / c) \times e^{j\Phi}, \quad (1)$$

where $\overset{o}{y}(\beta_\gamma,l)$ – array output signal at time moment l ; n – sensor number; N – amount of sensors; k – chip number; KT –amount of total components (chips); τ_e – chip length; d –distance between sensors; c – wave speed,

$$a(l) = \begin{cases} 1, & \text{if } 0 \le l \le \tau_e , \\ 0, & \text{if } 0 > l > \tau_e , \end{cases} \quad (2)$$

and

$$\Phi_k = \{+1,+1,+1,-1,+1,+1,+1,+1,-1,+1,+1,+1, \\ +1,-1,+1,-1,-1,-1,+1,-1,+1,+1,+1,-1,+1\} \quad (3)$$

are values of the binary phase-coded waveforms ($KT=25$).

It is easy to notice when $\beta_\gamma = 0$,

$$\overset{o}{y}(0,l) = N \cdot \sum_{k=0}^{KT-1} a(l - k\tau_e) \cdot e^{j\Phi_k} \qquad (4)$$

and the signal formed from the sensor, transmits the primary signal without any distortion (Fig. 3). In other cases, the situation is different. The magnitudes of the received waves at angles in the array are shown in Fig. 4 – 5.
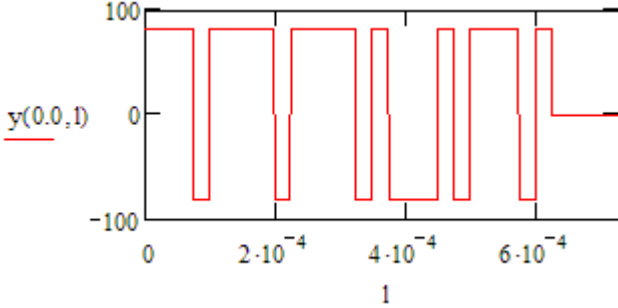

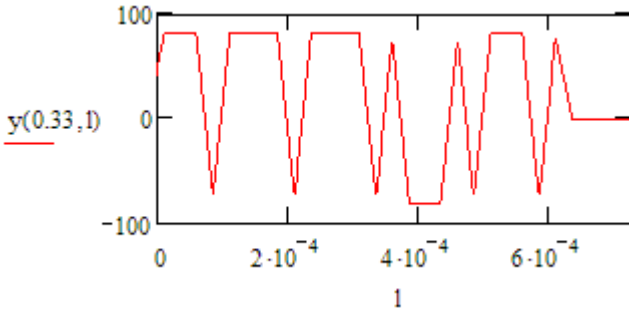**Fig. 3**. Array output at $\beta_\gamma = 0$ rad (Scanning signal)

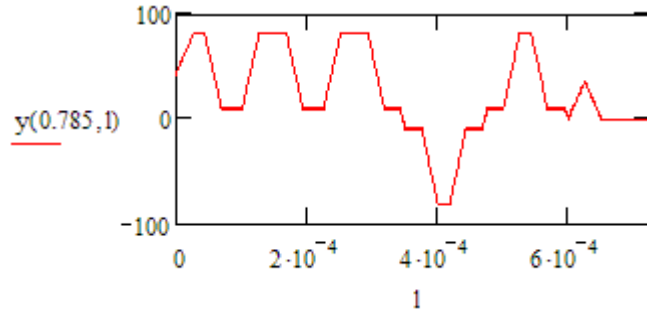**Fig. 4.** Array output at $\beta_\gamma = 0.33$ rad

Fig. 5. Array output at $\beta_\gamma = 0.785$ rad

As we can see, the increase of the receiving angle of the wave will cause a strong deformation in the form of the summary signal. The phase compensation array with much bigger length L_a than signal spatial length L_s (in our case chip spatial length inside the spread spectrum signal) does not work adequately when it receives signals at the directions that are deflected from the normal.[10]

Advanced FFT beamforming

One way to solve this problem is to use the compensation of time lags of the signal. In order to produce the correct time delay, we can use characteristics of Fourier transmission [11] [12]. For this purpose, we can create

digital data buffers behind each sensor and as a result obtain a two-dimensional data matrix M behind the sensor array. First, we must compute the complex frequency spectrum from each column n of the matrix M. Since the complex weight is a function of frequency q, an appropriate complex weight must be applied to each frequency component contained in the signal spectrum. This must be done at each sensor n in the array

$$\overset{o}{Y}_{n,(q+Lp)} = C(n,q) \cdot \frac{1}{L-1} \sum_{l=0}^{L-2} M_{l,n} \times$$

$$\times \exp\left(-j\frac{2\pi \cdot q \cdot l}{L-1}\right), \qquad (5)$$

where q – sampled frequency $q = \overline{-Lp, Lp}$, L – the amount of signal samples and $Lp = (L-2)/2$.

Complex weight $C(n,q)$ is expressed by the formula

$$C(n,q) = \begin{vmatrix} 0 \; if \; |n| > N-1 \; , \\ a(n,q) \cdot \exp(j\theta(n,q)) \cdot \exp(j\varphi(n)), \end{vmatrix} \qquad (6)$$

where $a(n,q)$ is the frequency dependent amplitude window. For time delay compensation we will use the weight

$$\theta(n,q) = \frac{2\pi q}{(L-1)} \cdot round\left(\frac{n \cdot d \cdot fs \cdot \cos(\beta_\gamma)}{c}\right) \qquad (7)$$

and for phase compensation the weight

$$\varphi(n) = 2 \cdot \pi \cdot n \cdot d \cdot \frac{\cos(\beta_\gamma)}{\lambda_0} . \qquad (8)$$
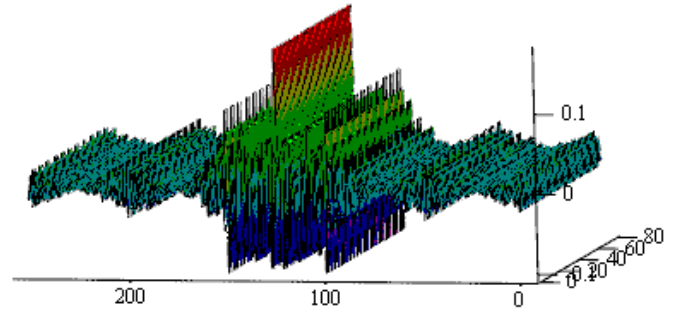

Fig. 6. Complex weighted frequency spectrum $Y_{n,(q+Lp)}$

It is important to notice that both weights (7), (8) must be used in order to achieve the correct time delay and phase compensation. The complex weighted frequency spectrum $Y_{n,(q+Lp)}$ is depicted in Fig.6 ($a(n,q) = 1, \forall n, \forall q$, N=81). Taking the inverse Fourier transform from $Y_{n,(q+Lp)}$ with respect to frequency q, the output electrical signals in each channel are now in phase and we obtain practically equivalent situation with $\beta_\gamma = 0$ (Fig. 3).

As an advantage, this method enables us to perform immediately an optimal reception to evaluate the actual round-trip time delay (optimal receiver must carry out the pattern of the function of uncertainty). In this case, it is

really not necessary to take the inverse Fourier transform and thus it helps to save system resources. Optimal reception in a frequency-domain is expressed with the formula

$$\psi(\tau,0) = \sum_{q=-Lp}^{Lp} \left[YS_{(q+Lp)} \cdot SKV_{(q+Lp)} \right] \times$$

$$\times \exp\left(j\frac{2\pi \cdot q \cdot \tau}{L-1} \right), \qquad (9)$$

where

$$YS_{(q+Lp)} = \sum_{n=0}^{N-1} \overset{o}{Y}_{n,(q+Lp)} ; \qquad (10)$$

$$SKV_{(q+Lp)} = \frac{1}{L-1} \sum_{l=0}^{L-2} \overset{o}{VTV}_l \times$$

$$\times \exp\left(j\frac{2\pi \cdot q \cdot l}{L-1} \right); \qquad (11)$$

$$\overset{o}{VTV}_l = N \cdot \sum_{k=0}^{KT-1} a(l-k\tau_e) \cdot e^{j\Phi_k} \qquad (12)$$

is the support signal. It is important to notice that all values of $SKV_{(q+LP)}$ can be previously saved into the processor memory. The appropriate optimal filter output is shown in Fig. 7.
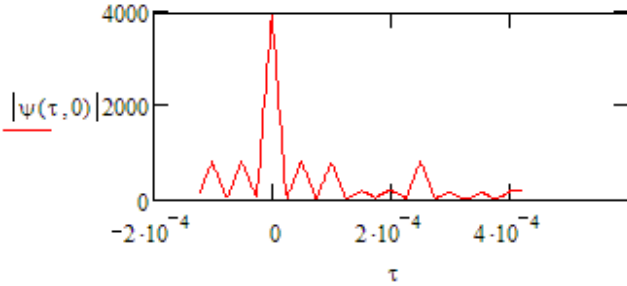

Fig. 7. Vertical cut of the ambiguity function of the optimal filter

Due to the fact that the imaginary parts of the complex weights can be selected independently and appropriately so that the beam-pattern of the beamformer is constant over the frequency band (i.e. frequency-invariant beamformer), while the amplitudes $a(n,q)$ in the complex weights are used to control the beam-pattern characteristics. The proposed method is able to control the main-beam width and sidelobe levels of the beam-pattern in a wide range of frequencies, providing a wideband non-adaptive method for reducing interference. In the case of a frequency-domain structure, it is insensitive to the sampling rate (required only at the Nyquist frequency).

Block-Phase Beamforming

Here we take into consideration that the amount of simultaneously activated sensors

$$N_{ef}(\beta_\gamma) = \left| \begin{array}{l} \dfrac{\tau_e \cdot c}{d \cdot |\cos(\beta_\gamma)|} \ if \ \cos(\beta_\gamma) \neq 0 , \\ N \ otherwise \end{array} \right. \qquad (13)$$

is determined by the spatial length of the signal smallest element of the signal. Sensor array is divided into subarrays [13] where the amount of sensors inside the of subarray is less or equal to $N_{ef}(\beta_\gamma)$.

The output signal in different partial directions β_γ can be computed with the formula

$$\overset{o}{y}(l,\beta_\gamma) = \sum_{i=0}^{grp(\beta_\gamma)-1} \sum_{n=\frac{i\cdot N}{grp(\beta_\gamma)}}^{\left(\frac{N\cdot(i+1)}{grp(\beta_\gamma)}\right)-1} \overset{o}{M}_{l+d(i,\beta_\gamma),n} \times$$

$$\times \exp\left(j\frac{2\pi \cdot n \cdot d \cdot \cos(\beta_\gamma)}{\lambda_0} \right), \qquad (14)$$

where $grp(\beta_\gamma)$ – the amount of subarrays corresponding on at different partial directions β_γ and i – the index of subarrays. In the case of $N=81$

$$grp(\beta_\gamma) = \left| \begin{array}{l} 1, if \ N_{ef}(\beta_\gamma) \geq N ; \\ 3, if \ 27 \leq N_{ef}(\beta_\gamma) < N ; \\ 9, if \ 9 \leq N_{ef}(\beta_\gamma) < 27 ; \\ 27, if \ 3 \leq N_{ef}(\beta_\gamma) < 9 ; \\ N \ otherwise . \end{array} \right. \qquad (15)$$

Delay (in samples) of the i-th subarray corresponding at on partial direction β_s is fixed by the formula

$$d(i,\beta_\gamma) = round\left(fs \cdot \frac{i \cdot N}{grp(\beta_\gamma)} \cdot \frac{d \cdot \cos(\beta_\gamma)}{c} \right). \qquad (16)$$

To reduce the amount of mathematical operations in real time, we can previously record all the values of $d(i,\beta_\gamma)$ and $grp(\beta_\gamma)$ into the system memory. Three-dimensional image of the two-dimensional delay array $d(i,\beta_\gamma)$ is shown in Fig. 8.

Vertical axis represents subarray delays in samples and horizontal axes represents subarray indexes and sampled directions. Fig. 9 shows the output signal of the sensor array if the falling angle of the signal is $\beta_\gamma = 0.524$ rad .
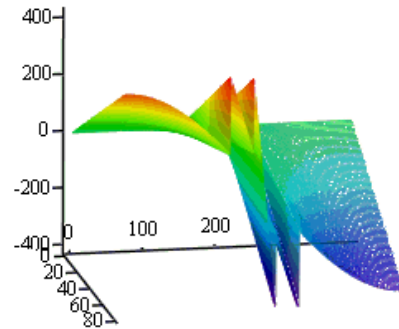

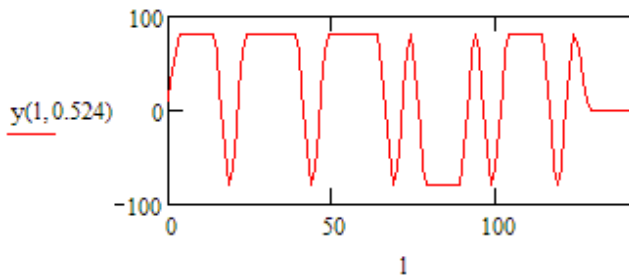**Fig. 8.** Three-dimensional image of $d(i,\beta_s)$

Fig. 9. Array output after the block-phase compensation

Fig. 10 shows the output signal after performing an optimal reception in the case of $\beta_\gamma = 0.524$ rad ($\beta_\gamma = \beta_{kr}$) with a support signal (12).
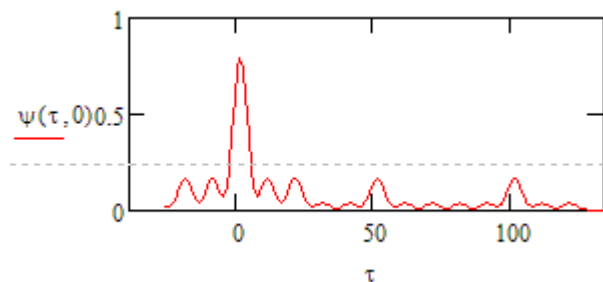

Fig. 10. Vertical cut of the ambiguity function of the optimal filter after block-phase compensation

The block-phase method does not give such good results as the previous method, but the results are still good and the required computing power is much lower compared with previous methods. When the scanning signal falls onto the array from the normal direction, only summing up of signal elements occurs in the system. When the signal falls onto the array at some abnormal angles, the sensor array is divided into sub (phase) arrays. Thereby, the required computing power even decreases compared to the classical phase arrays since the calculation of the Fourier transform is executed using smaller blocks.

Conclusions

According to the requirements, to reduce the impulse power and the precision of evaluating the time lag, the most effective method is to use signals based on the Barker's codes. It is possible to use LFSR-sequences, but in this case longer code sequences must be used to achieve the results equal to the Barker's codes. This aggravates the discovery of objects within nearer distances to the sensor array. We can get the most effective scanning signals when we use the nested codes, synthesized on the basis of Barker's codes, since these ensure extraordinarily narrow peak area and the same levels for the sidelobe as for the classical Barker's codes. A problem may arise with the spatial length of signals, which increases the minimal operating radius of the system. Therefore, when realizing the system in practice, it is reasonable to make the configuration of the choice of a scanning signal simpler. Concerning the dynamics of the scanning signals in the sensor array surveyed in the present work, we observed that the general behavioural model is the same and still connected with the duration of the shortest element of the signal. Some differences appeared when using very long nested codes (the average amplitude of the output signal of the sensor array remained somewhat higher for large angles than when using traditional signals) but for the dynamics, the choice of scanning signals is not an essential factor. The choice of the scanning signal is rather determined by the minimal and maximal operating radiuses and the correlation features of the signal.

The choice of an algorithm depends on concrete situations, available hardware, etc. Comparing the theoretical results it can be stated that they are all realizable and provide very good results theoretically. Essentially, the whole angular interval $\beta_\gamma = \pm 90^\circ$ can be reduced to the equivalent situation $\beta_\gamma = 0$. The compensation of lags in the frequency space can be considered the most appropriate approach, but still this method is quite resource consuming. The block phase method provides sufficiently good results if we stick to the rule that the relation $\beta_\gamma \leq \beta_{kr}$ is valid according to the spatial length of one element ("chip") of the signal and the length of the subarray. There is a minor loss in the level of the main lobe of the output signal of the optimal receiver, but this loss is insignificant. It is essential that the main lobe width and general shape of the optimal receiver do not change. The level of the sidelobes remains the same.

It must also be noted that the block phase method is not invariant to the scanning signal. Its concrete realization (the number of subarrays formed) is dependent upon the scanning signal (to be more exact upon the duration/spatial length of its shortest element). Since by dividing the sensor array into sub-arrays, the lengths of the Fourier transforms decrease, the processing of the whole array occurs more rapidly as compared to the case when the Fourier transform is calculated simultaneously for all the array elements.

The results of modelling enable us to draw the following conclusions:

1. Derived from the characteristic of the signal, the sensor array is not able to use classical phase compensation for the purposes of beam steering.
2. The block-phase method provides quite good quality and enables us to reduce the required computing power as compared with advanced FFT beamforming.
3. The most appropriate method seems to be advanced FFT beamforming.

References

1. International Hydrographic Organisation. Web address: http://www.iho.int/.
2. **David E. Wells, David Monahan.** IHO S44 Standards for Hydrographic Surveys and the Variety of Requirements for Bathymetric Data // The Hydrographic Journal. – 2002. – No. 104.
3. **IHO** Standards for Hydrographic Surveys (S-44), fourth edition // International Hydrographic Organisation. – Monaco. – 1998.
4. **Merrill I. Skolnik.** Radar handbook // Boston: McGraw-Hill, 1990.
5. **Mark A. Richards.** Fundamentals of radar signal processing // New York: McGraw-Hill, 2005.

6. **Arro I., Derkats J., Kozhevnikov V.** Ecologically Safe Multichannel Sonar System // ISPC 2003 Conference Proceedings. – Dallas, Texas, USA. – April 1-3 2003.
7. **Harry L. Van Trees.** Detection, estimation, and modulation theory: Radar-sonar signal processing and gaussian signals in noise // John Wiley & Sons, Inc. – 2001.
8. **Arro I., Duhnik A., Derkats J.** Interaction of the PSK signal with a phase array // Electronics and Electrical Engineering. – Kaunas: Technologija, 2002.
9. **Toomas Ruuben.** The dynamics of signals with spread spectrum in sensor arrays // UDT Europe 2002, Conference Proceedings, CD-rom. – La Spezia, Italy. – 18-20 June 2002.
10. **Ilmar Arro, Raivo Portsmuth, Toomas Ruuben.** High Resolution Multi-Beam Sonar // UDT Europe 2000, Conference Proceedings, CD-rom. – London, UK. – 26-29 June 2000.
11. **Lawrence J. Ziomek.** Fundamentals of Acoustic Field Theory and Space-Time Signal Processing // Boca Raton, Ann Arbor, London, Tokyo: CRC Press Inc, 1995.
12. **Tuan Do-Hong, Peter Russer.** Spatial Signal Processing for Wideband Beamforming // Proceedings of XII International Symposium on Theoretical Electrical Engineering (ISTET 2003). – July 2003. – P. 73–76.
13. **Arun K. Bhattacharyya.** Phased Array Antennas // Wiley-Interscience publication. – USA. – 2006.

T. Ruuben, J. Derkats. Some Methods of Signal Processing and Beamforming in a Hydrographic Applications // Electronics and Electrical Engineering. – Kaunas: Technologija, 2008. – No. 6(86). – P. 27–32.

Some signal processing and beamforming methods for hydrographic applications are presented. Some additional signals and processing methods as part of the bathymetric data collection to determine the new measurement techniques will be discussed. Optimal binary sequences are used for sounding signal generation, leading to an increase system resolution. The dynamics of the spread spectrum signals in sensor array models with the optimum reception methods will be described. The advanced FFT beamforming will be compared with the block-phase beamforming method in terms of the practical realization approach. Ill. 10, bibl. 13 (in English; summaries in English, Russian and Lithuanian).

Т. Руубен, Ю. Деркатс. Использование методов обработки сигналов в гидрографии // Электроника и электротехника. – Каунас: Технология, 2008. – № 6(86). – С. 27–32.

Представлены некоторые методы обработки сигналов и формирования луча, которые используются в гидрографии. Обсуждаются особенности методов при сборе батиметрических данных. Предлагаются новые методы измерения. Оптимальные двоичные последовательности используются для создания измерительного сигнала, что привдит к увеличению разрешения системы. Описана динамика сигналов распределенного спектра в моделях массивов датчиков с оптимальными методами приема. Инновационный метод формирования луча FFT сравнен с блокфазным методом формирования луча в терминах практического применения. Ил. 10, библ. 13 (на английском языке; рефераты на английском, русском и литовском яз.).

T. Ruuben, J. Derkats. Kai kurių signalų apdorojimo ir spindulio formavimo metodų taikymas hidrografijoje // Elektronika ir elektrotechnika. – Kaunas: Technologija, 2008. – Nr. 6(86). – P. 27–32.

Apžvelgti kai kurie hidrografijoje taikomi signalų apdorojimo ir spindulio formavimo metodai. Aptariamos metodų ypatybės, pasireiškiančios surenkant batimetrinius duomenis. Siūlomi nauji matavimo metodai. Gylio matavimo signalui generuoti naudojamos optimalios dvejetainės sekos. Tai leidžia padidinti sistemos skiriamąją gebą. Aprašomi paskirstytojo spektro signalų jutiklių masyvų modeliai, naudojantys optimalius priėmimo metodus. Pažangus FFT spindulio formavimo metodas lyginamas su blokiniu faziniu spindulio formavimo metodu, atsižvelgiant į praktinius pritaikymo ypatumus. Il. 10, bibl. 13 (anglų kalba; santraukos anglų, rusų ir lietuvių k.).